

Laser heterodyne system for measurement of minor constituents in the atmosphere

S L Jain

Radio and Atmospheric Sciences Division, National Physical Laboratory, New Delhi 110 012

Received 2 April 1996

The monitoring of greenhouse gases has an important role in the understanding of global change. The reporting of ozone depletion in general and ozone hole over Antarctica in particular witnessed an unprecedented surge of interest in the monitoring of various trace species. The infrared spectroscopy is a powerful tool for the investigation of atmospheric minor constituents. The laser heterodyne spectrometer due to its ultra-high spectral resolution and quantum limited sensitivity can resolve the individual spectral lines completely and has been used widely for atmospheric studies. A highly sophisticated laser heterodyne system using a 1 GHz hi-tech acousto-optic spectrometer has been designed and developed at NPL, New Delhi, for monitoring ozone and other related constituents in the atmosphere. The salient features of the laser heterodyne system and the acousto-optic spectrometer and the results obtained are reviewed in detail.

1 Introduction

The measurement of minor constituents in the atmosphere is of great significance to understand the physics, chemistry, dynamics and radiation budget of the atmosphere. The discovery of catalytic destruction of O_3 by ClO_x and NO_x in seventies by Johnston¹ in general and ozone hole phenomenon^{2,3} over Antarctic region during spring time in eighties in particular has generated an unprecedented surge of interest in the monitoring of ozone and other related minor constituents in the atmosphere. It is well known that our earth is shielded by a thin layer of ozone which saves it from the harmful effects of solar ultraviolet UV-B radiation, which besides having adverse impact on plants, agriculture and climate, is a primary cause of skin cancer. It has also been recognized that the greenhouse effect due to non CO_2 gases such as CFCs, N_2O , CH_4 , O_3 , etc. is as much as that due to CO_2 gas, while it was only due to CO_2 gas during the pre-industrial era. The increase of these greenhouse gases in the atmosphere may cause global warming which in turn may raise the sea level all over the world, affecting adversely the coastal cities and low lying countries such as Bangladesh, Netherlands, Maldives, etc. Therefore global measurement of vertical, horizontal and temporal distributions of various atmospheric gases has become essential.

Infrared spectroscopy has played a great role in the monitoring of most of the atmospheric minor constituents which have vibrational rotational

characteristic absorption lines in the infrared window (8-12 μm) region. Careful study of their spectra with high resolution techniques provides quantitative information about the concentration of various minor constituents. Infrared spectrometers have the capability to resolve individual spectral lines. For example, Michelson interferometers provide spectral resolving power of 10^4 - 10^5 . Laser heterodyne spectrometer has ultra-high spectral resolution (10^5 - 10^7) and quantum limited sensitivity^{4,5}. Therefore, it can reveal complete spectral line profiles even for Doppler-broadened absorption lines formed in the upper atmosphere. The capabilities of laser heterodyne system for monitoring of ozone and other related constituents in the atmosphere have been demonstrated by various investigators.

A highly sophisticated laser heterodyne system has been designed, developed and set up at National Physical Laboratory (NPL), New Delhi, to monitor various trace species in the troposphere and stratosphere during the Indian Middle Atmosphere Programme. The laser heterodyne system with 1 GHz acousto-optic spectrometer (AOS) as back end, after successful operation at NPL, was taken to Maitri, an Indian Antarctic station (lat. $70^\circ 46'S$, long. $11^\circ 44'E$), during the summer of 1993-94 and it has been operated there successfully to obtain ozone profiles; this system is the first of its kind used over Antarctic region. In the present communication the historical background of development of laser hetero-

dyne spectrometer, its salient features along with its automation using a hi-tech 1 GHz acousto-optic spectrometer, and the results obtained are reviewed.

2 Historical background

The term heterodyne has its roots in the Greek words heteros (other) and dynamis (force).

Heterodyne = (hetero + dyne) = Separate force

Super heterodyne = (Super sonic + heterodyne)

It is interesting to review the origin of the above two words and trace early history of heterodyne systems up to the first optical heterodyne experiment of 1955. The story started in 1902 with the issue of patent to Fessenden⁶ with simple title "wireless signalling". The invention was the concept of transmitting two separate radio frequencies, receiving the same on two separate antennas and mixing the two to produce an audio frequency. The "mixer" in this case was an iron core driving a telephone diaphragm and deflection was proportional to electrical power, thus yielding acoustic output at the difference frequency. It is not clear when the term "heterodyne" was coined but Hogan⁷ published a paper entitled "The heterodyne receiving system and notes on recent Arlington-Salem tests" in 1913 where it was suggested to transmit only one wave and generating the second frequency at the receiving station and this gave birth to local oscillator. In 1917 Armstrong⁸ carried out a thorough investigation of heterodyne phenomenon occurring in the oscillating state of the "regenerative electron relay". A major breakthrough in the field—the development of super heterodyne receiver—was achieved by Armstrong⁹ in 1921 and this famous invention is now used in systems as diverse as household AM radio receivers and microwave Doppler radars. The prefix "super" refers to "super audible frequency" that can be readily amplified.

The use of heterodyne in optical region took place in 1955. In a classical experiment Forrester *et al.*¹⁰ observed the mixing of two Zeeman components of incoherent visible spectral line in a specially constructed photomultiplier tube. The developments of laser by Maiman¹¹ in 1960, He-Ne laser at 1.15 μm by Javan *et al.*¹² and ruby laser at 0.6943 μm by McMurtry and Siegman¹³ observed the emergence of optical heterodyning. Teich *et al.*¹⁴ were the first to use CO₂ laser, at 10.6 μm in conjunction with a copper-doped germanium photoconductive detector operated at 4 K for heterodyne experiment. Frerking and Muehlner¹⁵ were the first investigators to succeed in measuring solar absorption spectra of atmos-

pheric ozone around 1010 cm^{-1} using a tunable diode laser. Abbas *et al.*¹⁶ observed ozone vertical profiles with CO₂ laser heterodyne. Subsequently the laser heterodyne systems using either CO₂ laser or tunable semiconductor diode laser have been used by various investigators¹⁷⁻³³ for measuring atmospheric minor constituents such as O₃, N₂O, NH₃, ClO, HNO₃, water vapour, etc., wind velocity^{34,35}, drawing temperature profiles, and also for studying the atmospheres of various other planets such as Venus, Jupiter and Mars (Refs 36-38).

3 Principle of operation

The operation of laser heterodyne receiver is based on square law response of the photodetector to the incident electric field. The two electromagnetic waves of different frequencies (ν_1 and ν_2) mix at the photo device to produce a signal at difference frequency $\nu_1 - \nu_2$, when one of these beams is strong (called local oscillator beam) and the sensitivity for the process is considerably greater than that of direct detection because of the high conversion gain between power at the input and at the difference frequency³⁹. In addition to high conversion gain the heterodyne detection exhibits both strong directivity and high frequency selectivity. The high frequency selectivity in turn permits the noise bandwidth to be reduced to a very small value. Some of the characteristics of the laser heterodyne radiometer are discussed below:

3.1 Signal-to-noise ratio

The signal-to-noise (S/N) ratio for the thermal source (black body) which fills the mixer's field of view is given by⁴⁰

$$S/N = \eta (B_{iv} t)^{0.5} \tau [\exp(h\nu/kT) - 1]^{-1}$$

where η is the quantum efficiency, B_{iv} the IF bandwidth, t the integration time, h the Planck's constant, ν the frequency, k the Boltzmann constant, T the black body temperature, and τ the transmittance of the media between the source and the mixer.

For the transparent atmosphere at 10 μm , if the bandwidth $B_{iv} = 25$ MHz, integration time $t = 10$ s and $\eta = 0.5$, the signal-to-noise ratio is found to be 10⁴ or 40 dB. The atmospheric effects, optical losses, polarization, chopper, etc. will degrade the value of S/N by an order of magnitude. The S/N with the same parameters was computed for visible (0.6 μm) range and found to be 10⁻⁴ or -40 dB, which suggests that heterodyne system is particularly suited for infrared radiations.

3.2 Noise equivalent power (NEP)

The NEP for laser heterodyne system at $10\ \mu\text{m}$, $\eta=0.5$ and $B_{iv}=1\ \text{MHz}$ is given by $9 \times 10^{-17} (1/t)^{0.5}\ \text{W}$, while NEP for direct detection system for the same parameters is given by $10^{-12} (1/t)^{0.5}\ \text{W}$. This computation shows that heterodyne system is four orders of magnitude more sensitive than the direct detection.

3.3 Spectral resolution

The laser heterodyne system is well suited for atmospheric studies because of its ultra-high spectral resolution. One can get resolution of the order of $0.00017\ \text{cm}^{-1}$, i.e. $5\ \text{MHz}$ at $10\ \mu\text{m}$.

3.4 Detection sensitivity

The minimum detectable column density for solar absorption mode using laser heterodyne system is $4 \times 10^{13}\ \text{cm}^{-2}$ and minimum detectable volume mixing ratio is around 10^{-12} (for absorption coefficient $50\ \text{cm}^{-1}\ \text{atm}^{-1}$, $B_{iv} = 5\ \text{MHz}$, $t=1000\ \text{s}$). Thus the sensitivity of IR laser heterodyne system is of the order of mixing ratio of around 10^{-12} , which shows that most of the minor constituents in the atmosphere can be detected by this type of system.

4 Experimental set up

4.1 Laser heterodyne system

Infrared laser heterodyne spectroscopy pro-

vides a powerful tool for identification of weak molecular and atomic species. The advantages of the laser heterodyne system over other techniques are its ultra-high spectral resolution, high spatial resolution, high quantum detection efficiency, and very good signal-to-noise ratio. The high resolution makes the system very selective as the interference problem due to overlapping lines or bands are minimized and the lines can be resolved completely with high resolution unlike with the other techniques.

The block diagram of the system designed, developed and set up at NPL, New Delhi, is depicted in Fig. 1. The CO_2 laser used as a local oscillator is tuned on a line corresponding to the absorption line of the minor constituent of interest. The solar tracker (heliostat) follows the sun and brings in the solar radiation. The incoming chopped solar radiation is filtered out and IR radiation ($8\text{--}12\ \mu\text{m}$) and CO_2 laser beam of moderately low power are combined via a zinc selenide beam splitter. The solar radiation and CO_2 laser beam are co-aligned and focussed on the high speed liquid nitrogen cooled HgCdTe detector which acts as a mixer as well as narrow band filter. The detected signal is nothing but the difference frequency (IF). The IF signal is further amplified in low noise, wide band ($5\text{--}1200\ \text{MHz}$) RF amplifiers and passed through various RF filter channels ($25\text{--}1200\ \text{MHz}$). The signal from various

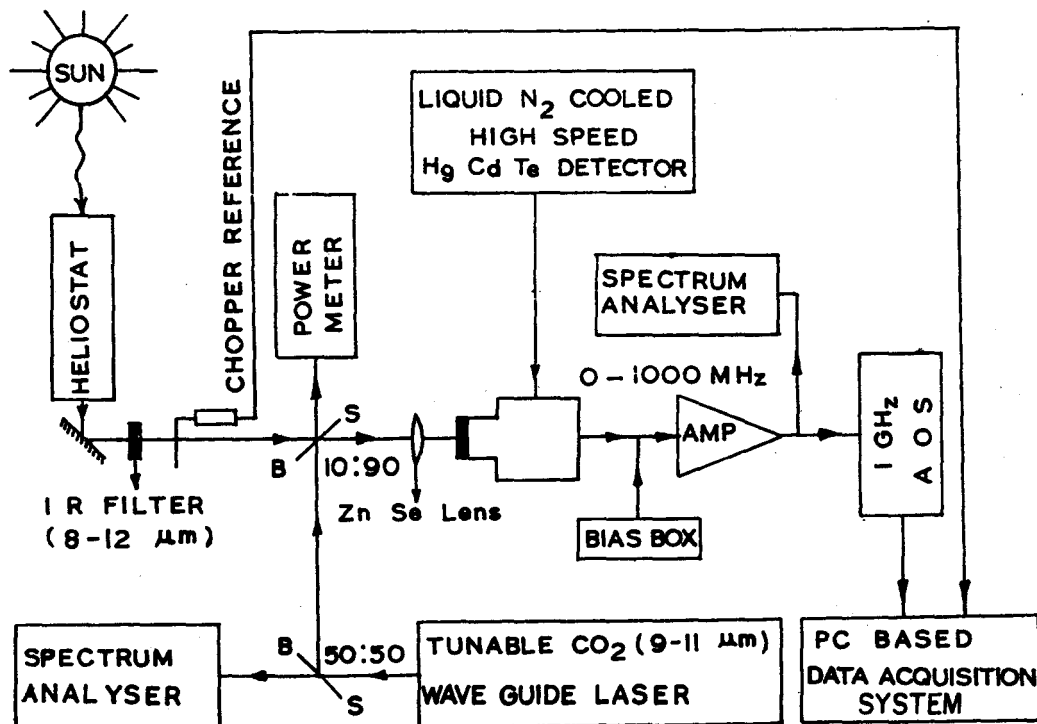


Fig. 1—Block diagram of laser heterodyne system of NPL, New Delhi.

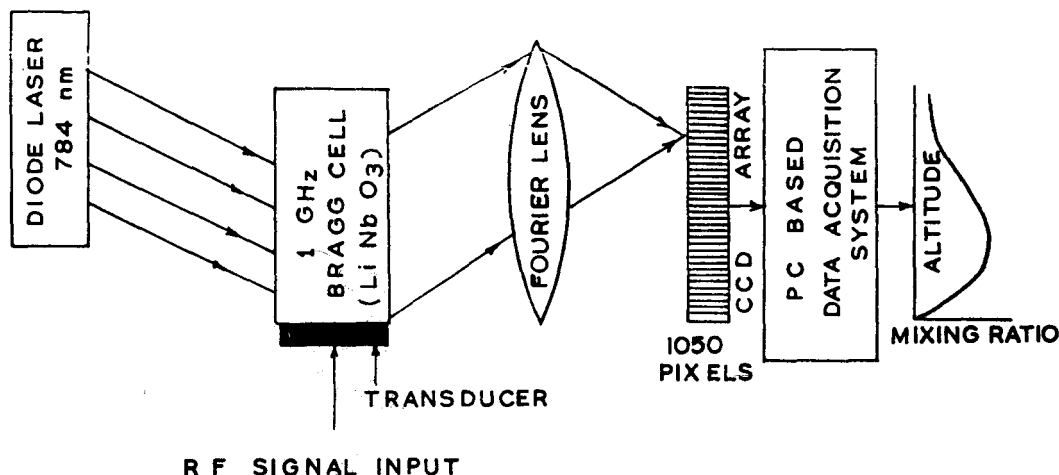


Fig. 2—Block diagram of acousto-optic spectrometer.

channels is square law detected and is fed to lock-in amplifier where synchronous detection takes place. The signal can be read directly from the lock-in amplifier or recorded on a strip chart recorder. The observations taken at different frequency channels in the wing of the absorption line of the minor constituent of interest would resolve the line completely and vertical profiles can be obtained with these data using inversion technique. The number of points in the wing of the line would decide the height resolution. The system has been described in detail elsewhere²⁰⁻²⁴. Till now this system was being operated manually by tuning various RF filters (25-1200 MHz), but this process was time consuming and amenable to errors in the measurements. To overcome these drawbacks, the system has been made semi-automatic by incorporating a wide band acousto-optic spectrometer described below.

4.2 Acousto-optic spectrometer (AOS)

Acousto-optic technique for power spectral measurements has been exploited for a variety of signal analysis applications⁴¹⁻⁴⁶. The spectrum analysis is one of the most useful techniques in modern science and virtually every discipline makes use of it in one form or the other. Although the architecture may vary depending upon the acousto-optic (AO) signal processing function, the common ingredients in these systems are an optical source which may be a laser diode or visible emitting gas laser, a light modulator consisting of one or more AO Bragg devices, and an array of photodetectors. The Bragg cell, also known as AO diffraction cell, serves the key role in an acousto-optic spectrometer. It converts RF signals to ultrasonic travelling waves which modulate the optical index of the cell. The cell is illuminated

across its aperture by a laser beam. A fraction of light is diffracted by acoustic waves, the angle of diffraction is determined by the frequency while the intensity of the diffracted light is proportional to the power of the input RF signal. The intensity distribution can be detected by linear array of photodetectors which in turn represent the required RF power spectrum.

An acousto-optic spectrometer with 1 GHz bandwidth has been designed and developed in collaboration with Meudon Observatory, France, and integrated with the laser heterodyne system developed at NPL, New Delhi. The block diagram of the acousto-optic spectrometer is shown in Fig. 2. The system consists of 1 GHz Bragg cell (Li Nb O₃), a diode laser emitting at 784 nm, a Fourier lens, a 1050 pixel CCD array, and a PC-based data acquisition system. Proper software and hardware have been developed to digitize the frequency power spectrum for further analysis and for getting height profiles of various minor constituents.

The acousto-optic spectrometer developed has been tested with a laser heterodyne system of Reims University, France. The frequency power spectra obtained using an empty cell of 200 cm length and 600 m Torr ozone in the cell are as expected. The P(24) CO₂ laser line in 9.6 μm band was used. The spectrum thus obtained shows very well defined ozone absorption lines. A spectral resolution better than 5 MHz has been obtained. A typical ozone line spectrum obtained over Maitri, Antarctica, during February 1994 is depicted in Fig. 3. The use of AOS as back end of laser heterodyne system is timely and well suited to detection of weak signals buried in noise. The main advantages of AOS are wide bandwidth, high resolution, large number of channels,

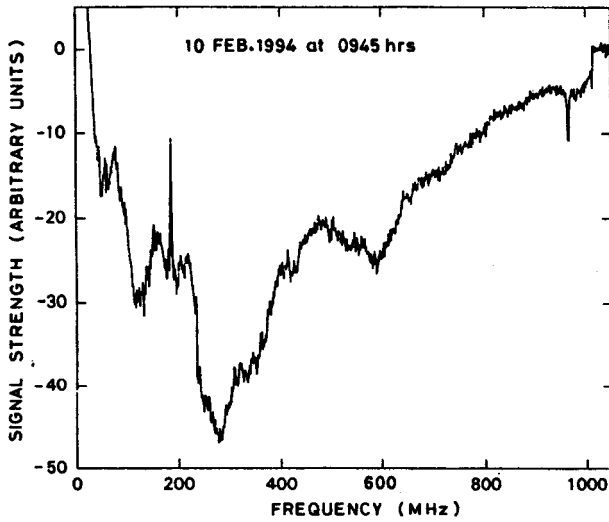


Fig. 3—Line spectra of ozone observed at Maitri, Antarctica, on 10 Feb. 1994.

high detection sensitivity and compactness, light weight, and better energy efficiency.

5 Inversion technique

The composition or temperature profiles can be obtained by analysing individual spectral lines measured at ultra-high spectral resolution through inverse solution of radiative transfer equation⁴⁷⁻⁵⁸ given below:

$$I_{\nu}(P, T) = B_{\nu}(T_s) \tau(\nu, P) + \int_{z_1}^{z_2} B_{\nu}(T) K(P, T) dz \quad \dots (1)$$

where

I_{ν} Emergent spectral intensity from a non-scattering atmosphere

$B_{\nu}(T_s)$ Planck's function at source temperature T_s

$\tau(\nu, P)$ Transmittance from surface to the top of the atmosphere

$K(P, T)$ Weighting function

$$K(P, T) = d\tau_{\nu} / dz \quad \dots (2)$$

$$z = -\ln P$$

The first term in Eq. (1) is the surface contribution, whereas the second term represents the atmospheric contribution to the spectral intensity. In the ground-based measurements of the earth's atmosphere in solar absorption mode, the second term, i.e. self-emission term in radiative transfer equation, is negligible as compared to solar surface contribution and the observed spectral intensity may be written as

$$I_{\nu}(P, T) = B(\nu, T_s) \tau(\nu, P) \quad \dots (3)$$

The atmospheric transmittance factor τ_{ν} may be given as

$$\tau(\nu, P) = \exp[-\int \sum_i k_{\nu i} du_i] \quad \dots (4)$$

where $k_{\nu i}$ is the specific absorption coefficient and du_i is the element of column density for the i th species of the absorbing gases given by

$$du_i(P) = q_i(P/P_0) (T_0/T) \sec \chi_z dz \quad \dots (5)$$

where q_i is the volume mixing ratio of the gas, χ_z is the solar zenith angle and subscript 0 refers to the reference quantities.

The spectral intensity I_{ν} from planetary atmosphere is measured for an appropriately chosen set of frequencies for which weighting functions $k_{\nu i}$ are well distributed over the atmosphere. The atmospheric composition profiles may be obtained through inverse solution of Eq. (2) if the temperature and pressure profiles are known.

The absorption coefficients $k(\nu)$ at line centre and in the wing of the line are calculated using the expression

$$k(\nu) = [S(T)/\pi] \cdot [\alpha / \{(\nu - \nu_0)^2 + \alpha^2\}] \quad \dots (6)$$

where

$$\alpha = \alpha_0 (P/P_0) (T_0/T)^{1/2} \quad \dots (7)$$

$$S(T) = S_0 (T_0/T)^{3/2} \times \exp\{1.439 E'' [(T - T_0)/T T_0]\} \quad \dots (8)$$

and α_0 is the line half-width at $T_0 = 298$ K, S_0 the line strength at T_0 , and E'' the lower energy level of transition.

The line parameters such as α_0 , S_0 , E'' , etc. are taken from HITRAN database 1986 edition⁵⁹. The line shapes are generally expressed by the Voigt function which is a convolution of Lorentzian and Gaussian functions. The former is an expression for pressure-broadened line shape which dominates in the troposphere and latter is that for Doppler-broadened line shape which dominates in the upper stratosphere and above. In the present case Lorentz profile was used below 25 km and Voigt profile above 25 km. The Voigt line shapes can be expressed as

$$k(\nu) = (S/\alpha') (y/\pi) \times \int_{-\infty}^{\infty} \exp[-t^2 / (y^2 + (x-t)^2)] dt \quad \dots (9)$$

where

$$\alpha' = (\ln 2/\pi)^{1/2} \quad \dots (10)$$

$$x = (\nu - \nu_0) (\ln 2)^{1/2} / \alpha_D \quad \dots (11)$$

$$y = \alpha (\ln 2)^{1/2} / \alpha_D \quad \dots (12)$$

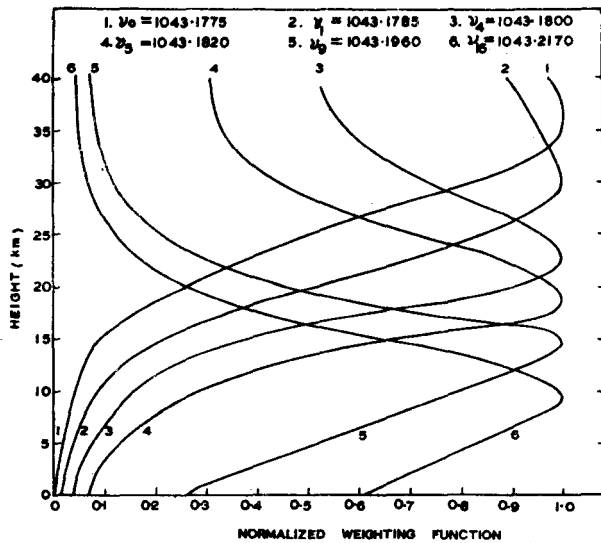


Fig. 4—Normalized absorption coefficients for different channels at the line centre and in the wing of the line as a function of altitude.

$$\alpha_D = 3.58 \times 10^7 (T/M)^{1/2} \text{ cm}^{-1} \quad \dots (13)$$

M Molecular weight

α Collision broadening

For the present analysis a careful selection of ozone absorption line $1043.1775 \text{ cm}^{-1}$ was made to get sharp weighting functions and hence height resolution. The weighting functions, which depend upon absorption coefficients, have a property of reaching maximum peak at different heights for different values of frequencies, i.e. at line centre and in the wing of the line as shown in Fig. 4. The line parameters such as half-width, line strength and lower state energy for ozone absorption line $1043.1775 \text{ cm}^{-1}$ are as follows: $\alpha_0 = 0.083 \text{ cm}^{-1}$, $S_0 = 1.050 \times 10^{-23} \text{ cm}^{-1} \text{ atm}^{-1}$, and $E'' = 26 \text{ cm}^{-1}$.

The line half-widths calculated for this line at various heights using Lorentz, Doppler and Voigt profiles are shown in Fig. 5. The computations were made at line centre and in the wing of the line. In all 16 channels were selected. It is to be noted that weighting functions computed peaks at different altitudes for each frequency channel and the sharpness decides the height resolution. The typical normalized absorption coefficients for ozone line centre ($1043.1775 \text{ cm}^{-1}$) and other frequency channels in the wing of the line are shown in Fig. 4.

The inversion technique developed at NPL for retrieval of ozone profiles was tested using model ozone profile⁶⁰. The spectral intensity computed using the above model ozone profile and line par-

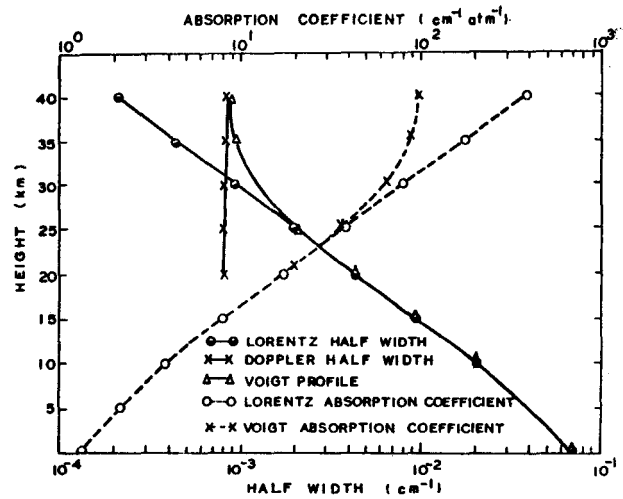


Fig. 5—Line half-widths and absorption coefficients for ozone obtained using Lorentz, Doppler and Voigt profiles.

ameters for $1043.1775 \text{ cm}^{-1}$ for each channel has been designated as I'_v . This computed spectral intensity at various frequency channels is the contribution of ozone at different altitudes and is used to retrieve height profiles for ozone using the iterative inversion method first suggested by Chahine⁴⁹ for remote sensing of atmospheric temperature by satellite observations and later developed by Abbas *et al.*^{55,56} and Jain^{57,58} for remote sounding of atmospheric minor constituents using high spectral resolution techniques. The inversion is carried out by the following steps:

(1) To start with, a uniform vertical distribution of mixing ratio of ozone, say 3 ppm, is guessed and this spectral intensity I'_v for each channel is computed corresponding to initial guess profile.

(2) I'_v and I_v are compared and residual R^n is computed by

$$R^n = (I'_v - I_v) / I'_v \quad \dots (14)$$

If the residual is zero or of the order of noise level of the measurement, the initial guess is the solution.

(3) If the residual is not zero, an improved mixing ratio at levels corresponding to the peaks of absorption coefficients is obtained from the relaxation equation

$$q^{n+1}(P_j) = \alpha_j q^n(P_j) \quad \dots (15)$$

where q^n and q^{n+1} are the n th and $(n+1)$ th guesses, α_j is the scaling factor and P_j is the pressure at level j .

(4) The iteration process is repeated until each

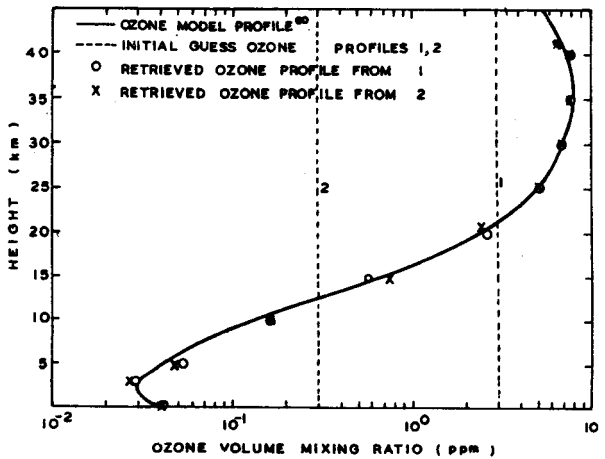


Fig. 6—Model and retrieved ozone height profiles obtained using inversion technique (normal case).

scaling constant approaches unity which is equivalent to satisfying the residual given by Eq. (15).

5.1 Case 1 : Normal ozone profile

In this case the model ozone profile⁶⁰ was used for testing the inversion technique developed at NPL. The retrieved profile obtained after 20 iterations is shown in Fig. 6. The retrieved profile compares well with that of original assumed profile. The inversion technique was further tested with different initial guess profiles having uniform vertical mixing ratio of 0.3 ppm, 3 ppm, etc. and each time the retrieved profile compared well with the original one, which demonstrated that the retrieved profile is independent of the initial guess profile as shown in Fig. 6. The complete profile is obtained with appropriate interpolation and extrapolation.

5.2 Case 2 : Ozone hole condition

The sensitivity of the inversion technique during very low values of ozone in 12-22 km height range due to the development of ozone hole was also tested. For these computations the ozone profile obtained at McMurdo station on 20 Oct. 1989 (Ref. 61), as shown in Fig. 7, was used. A similar method for retrieval of ozone profile as explained above was used for ozone hole conditions and it is found that after 20 iterations the retrieved ozone profile compares well with that of original, as shown in Fig. 7. In this case also the technique was tested for different initial guess profiles and found to be independent of them.

The above analysis shows that laser heterodyne system provides an important tool for monitoring ozone height profiles using inversion technique during both normal and ozone hole conditions

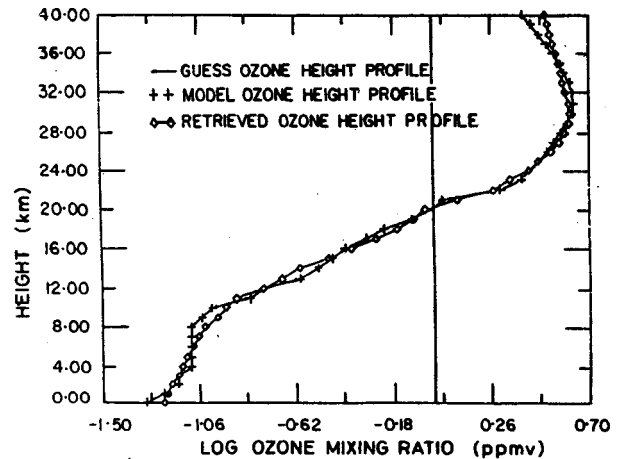


Fig. 7—Antarctica model profile⁶¹ and retrieved ozone profile obtained using inversion technique (ozone hole case).

over tropical latitudes as well as over Antarctica with height resolution of 2 to 5 km. Using laser heterodyne system at NPL, New Delhi, the efficiency of the inversion technique has been tested successfully to obtain vertical profiles of various trace species in the atmosphere such as O_3 , H_2O and NO_2 . The same system has the capability to monitor other trace species in the atmosphere by selecting appropriate absorption lines and by incorporating suitable changes in the inversion technique. The accuracy of the inversion technique will depend to a great extent on the accuracy of the line parameters which still needs extensive research work. The present system cannot be used during night and on cloudy days as it uses sun as the source.

6 Results and discussion

The laser heterodyne system is being used to get vertical profiles of ozone. The absorption line selected is $1043.1775 \text{ cm}^{-1}$. A large number of vertical profiles for ozone in the height range 15-40 km have been retrieved from the data using inversion technique⁵⁷. The ozone profiles obtained by laser heterodyne system at NPL were also compared with those obtained by balloon at Aya Nagar, India Meteorological Department, New Delhi (Ref. 62) on the days when data were available for both the systems. The two sets of profiles compare well within the experimental error. One typical example for 10 Feb. 1988 is shown in Fig. 8. A mean profile from all the data obtained by laser heterodyne system has also been prepared and compared with the mean profiles of the data obtained by balloon ozonesonde at Aya Nagar, New Delhi, and by rocket and balloon ozonesondes⁶³ at Thumba (Fig. 9). The mean

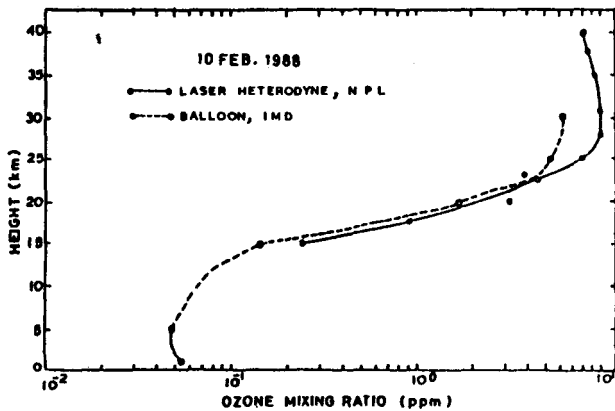


Fig. 8—Comparison of ozone mixing ratio profiles obtained by laser heterodyne system at NPL, New Delhi, and by balloon at Aya Nagar, IMD, New Delhi, on 10 Feb. 1988.

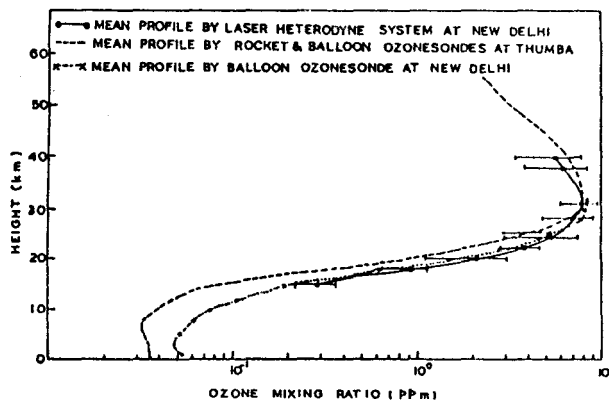


Fig. 9—Comparison of mean ozone vertical profiles obtained by (a) laser heterodyne system at NPL, New Delhi, (b) balloon ozonesonde at Aya Nagar, New Delhi, and (c) rocket and balloon ozonesondes at Thumba.

profiles at New Delhi by laser heterodyne system and balloon ozonesonde compare well but the values of ozone mixing ratio over Thumba are slightly less below the peak and more above the peak. This may be attributed to the latitudinal differences of the two places of measurements. As mentioned earlier, the laser heterodyne system was also deployed for the first time at Maitri, Antarctica, during the summer of 1993-94 to monitor vertical profiles of ozone. A typical ozone profile obtained over Maitri, Antarctica on 10 Feb. 1994 is depicted in Fig. 10.

The laser heterodyne system set up at NPL has demonstrated successfully its capability to monitor ozone height profiles in the atmosphere. Efforts are on to extend the facility to monitor other constituents such as NH_3 , SO_2 , CFCs, etc. to understand the complex interaction between atmospheric dynamics, chemistry and radiation budget, which in turn will require a large data base on regular basis at tropical as well as at Antarctic latitudes.

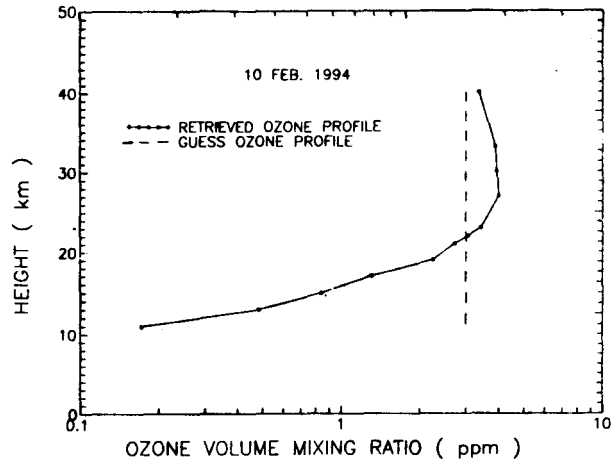


Fig. 10—Ozone profile obtained by laser heterodyne system on 10 Feb. 1994 over Maitri, Antarctica.

Acknowledgements

The author is grateful to Prof. E S R Gopal, Director, Dr B M Reddy and Dr K K Mahajan, Head RASD, NPL, for their keen interest and encouragement during the progress of the work. He also expresses his thanks to the Department of Ocean Development, Government of India, New Delhi, and the Indo-French Center for Promotion of Advanced Research, New Delhi, for financial support.

References

- 1 Johnston H S, *Science (USA)*, 173 (1971) 517.
- 2 Farman J C, Gardiner B G & Shanklin J D, *Nature (UK)*, 315 (1985) 207.
- 3 Stolarski R S, Krueger A J, Schoeberl M R, McPeters R D, Newman P A & Alpert J C, *Nature (UK)*, 322 (1986) 808.
- 4 Blaney T G, *J Atmos Sci (USA)*, 27 (1975) 960.
- 5 Menzies R T, *Laser Monitoring of Atmosphere*, edited by E D Hinkley, Chap. 7 (Springer, New York), 1976.
- 6 Fessenden R A, US Pat No. 706,740, August 1902.
- 7 Hogan J L, *Proc IRE (USA)*, 1 (1913) 75.
- 8 Armstrong E H, *Proc IRE (USA)*, 5 (1917) 145.
- 9 Armstrong E H, *Proc IRE (USA)*, 9 (1921) 3.
- 10 Forrester A T, Gudmundsen R A & Johnson P O, *Phys Rev (USA)*, 99 (1955) 1691.
- 11 Maiman T H, *Nature (UK)*, 187 (1960) 493.
- 12 Javan A, Ballik E A & Bond W L, *J Opt Soc Am (USA)*, 52 (1962) 96.
- 13 McMurtry B J & Siegman A E, *Appl Opt (USA)*, 1 (1962) 51.
- 14 Teich M C, Keyes R J & Kingston R H, *Appl Phys Lett (USA)*, 9 (1966) 357.
- 15 Frerking M A & Muchlner D J, *Appl Opt (USA)*, 16 (1977) 626.
- 16 Abbas M M, Kastiuk T, Mumma M J, Buhl D, Kunde V G & Brown L W, *Geophys Res Lett (USA)*, 5 (1978) 317.
- 17 Okano S, Taguchi M & Fukunishi H, *Geophys Res Lett (USA)*, 16 (1989) 551.
- 18 Glenar D, Kostiuk T, Jennings D E, Buhl D & Mumma M J, *Appl Opt (USA)*, 21 (1982) 253.

- 19 Hoell J M, Harward C N & Lo W, *Opt Eng (USA)*, 21 (1982) 320.
- 20 Hoell J M, Harward C N & William B S, *Geophys Res Lett (USA)*, 7 (1980) 313.
- 21 Fukunishi H, Okano S, Taguchi M & Ohnuma T, *Appl Opt (USA)*, 29 (1990) 2722.
- 22 Jain S L & Arya B C, *J Opt (India)*, 16 (1987) 102.
- 23 Jain S L, *Indian J Radio & Space Phys*, 18 (1989) 175.
- 24 Jain S L, *Proceedings of the National Workshop on ozone* (Indian National Science Academy, New Delhi), 1987, p. 77.
- 25 Peyton B J, Dinardo A J, Kanischak G M, Armar F R, Lange R A & Sard E W, *IEEE J Quantum Electron (USA)*, 8 (1972) 252.
- 26 Menzies R T & Chahine M T, *Appl Opt (USA)*, 13 (1974) 2840.
- 27 Menzies R T, *Geophys Res Lett (USA)*, 6 (1979) 151.
- 28 Menzies R T & Seals R K, *Science (USA)*, 197 (1977) 1275.
- 29 Mumma M J, Kostiuk T & Buhl D, *Opt Eng (USA)*, 17 (1978) 50.
- 30 Kostiuk T & Mumma M J, *Appl Opt (USA)*, 22 (1983) 2644.
- 31 Thiebeaux C, Courtois D, Delahaique A, Corre H Le, Mouanda J C & Fayt A, *Appl Phys (Germany)*, B47 (1988) 863.
- 32 Taquchi M, Okano S & Fukunishi H, *J Meteorol Soc Jpn (Japan)*, 68 (1990) 79.
- 33 Mouanda J C, Courtois D & Thiebeaux C, *Appl Phys (Germany)*, B57 (1993) 119.
- 34 Huffaker R M, *Appl Opt (USA)*, 9 (1970) 1026.
- 35 Bilbro J W, *Opt Eng (USA)*, 19 (1980) 535.
- 36 Betz A L, Johnson M A, McLaren R A & Sutton E C, *Astrophys J Lett (USA)*, 208 (1976) 141.
- 37 Betz A L, McLaren R A, Sutton E C & Johnson M A, *Icarus (USA)*, 30 (1977) 650.
- 38 Johnson M A, Betz A L, McLaren R A, Sutton E C & Townes C H, *Astrophys J Lett (USA)*, 208 (1976) 145.
- 39 Siegman A E, *Proc IEEE (USA)*, 54 (1966) 1350.
- 40 McElroy J H, *Appl Opt (USA)*, 11 (1972) 1619.
- 41 Turpin T M, *Proc IEEE (USA)*, 69 (1981) 79.
- 42 Borsuk G M, *Proc IEEE (USA)*, 69 (1981) 100.
- 43 Gordon E I, *Proc IEEE (USA)*, 54 (1966) 1391.
- 44 Kellman P, Shaver H N & Murray J W, *Proc IEEE (USA)*, 69 (1981) 93.
- 45 Noë J D L, Baudry A, Péralut M, Dierich P, Monnanteuil N & Colmont J M, *Planet & Space Sci (UK)*, 31 (1983) 737.
- 46 Noë J D L, Brillet J, Turati C, Mégie G, Godin S, Pelon J, Marché P, Barbe A, Gibbins C J, Dawkins A W J & Matthews, *Planet & Space Sci (UK)*, 35 (1987) 547.
- 47 Kaplan L D, *J Opt Soc Am (USA)*, 49 (1959) 1004.
- 48 Chahine M T, *J Opt Soc Am (USA)*, 58 (1968) 1634.
- 49 Chahine M T, *J Atmos Sci (USA)*, 27 (1970) 960.
- 50 Chahine M T, *J Atmos Sci (USA)*, 29 (1972) 741.
- 51 Colin L, *Mathematics of inversion*, NASA Rep TMX-62-150, 1972.
- 52 Deepak A, *Inversion method in atmospheric remote sounding* (Academic Press, New York), 1977.
- 53 Majumdar A K, Menzies R T & Jain S L, *Appl Opt (USA)*, 20 (1981) 505.
- 54 McElroy J H, *Appl Opt (USA)*, 11 (1972) 1619.
- 55 Abbas M M, *J Geophys Res (USA)*, 84 (1979) 4387.
- 56 Abbas M M, Shapiro G L & Alvarez J M, *Appl Opt (USA)*, 20 (1981) 3755.
- 57 Jain S L, *Indian J Radio & Space Phys*, 16 (1987) 324.
- 58 Jain S L, *Indian J Radio & Space Phys*, 18 (1989) 103.
- 59 Rothman L S, Camache R R, Goldman A, Brown L R, Toth R A, Pickett H M, Poynter R L, Flaud J M, Camy-Peyret C, Barbe A, Husson N, Rinsland C P & Smith M A H, *Appl Opt (USA)*, 26 (1987) 4058.
- 60 Kruezer A J & Minzner R A, *J Geophys Res (USA)*, 81 (1976) 4477.
- 61 Deshler T, Hofman D J, Hereford J V & Sutter C B, *Geophys Res Lett (USA)*, 17 (1990) 151.
- 62 Kulsrestha S M (IMD, New Delhi), Private communication, 1988.
- 63 Subbaraya B H, *Indian J Radio & Space Phys*, 16 (1987) 25.